12-2019

Role of Topoisomerase II alpha in DNA Topology and T cell responses during Chronic Viral Infections

Stella Chinyere Ogbu
East Tennessee State University

Role of Topoisomerase II alpha in DNA Topology and T cell Responses during Chronic Viral Infections

---

A thesis

presented to

the faculty of the Department of Biological Sciences and Internal Medicine

East Tennessee State University

In partial fulfillment

of the requirement for the degree

Master of Science in Biology

---

by

Stella Chinyere Ogbu

December 2019

Dr. Zhi Q. Yao, Chair

Dr. Shunbin Ning

Dr. Ling Wang

Keywords: Topoisomerase II alpha, DNA topology, DNA damage response, HIV, HBV, HCV, T cell dysfunction

ABSTRACT

Role of Topoisomerase II alpha in DNA Topology and T cell Responses during Chronic Viral Infections

by

Stella Chinyere Ogbu

The clearance of viruses is largely dependent upon the activation of T cells to generate a robust immune response. However, host responses are suppressed during chronic viral infections. In this thesis, we explored the role of Top2α in DNA topology in individuals with chronic HBV, HCV, and HIV infections. We found that Top2α protein expression and activity were low in T cells derived from chronically virus-infected individuals compared to healthy subjects. Using $CD4^+$ T cells treated with Top2α inhibitor or poisoner as a model, we demonstrated that Top2α inhibition disrupts the DNA topology, suppresses DNA repair kinase (ATM), and telomere protein (TRF2) expression, and induces T cell dysfunction. These findings reveal that Top2α inhibition is a mechanism by which viruses evade the host responses and establish persistent infection, and thus, restoring Top2α levels could be a way of boosting immune responses during chronic viral infections.

DEDICATION

This thesis is dedicated to my mum Dr. Catherine Uchendu-Ogbu. Thanks for your unrelenting love and support to me. I appreciate you.

ACKNOWLEDGMENTS

I would like to first thank my mentor, Dr. Zhi Qiang Yao, for his guidance and patience throughout my master's program at East Tennessee State University. I would also like to express my gratitude to the members of my committee, Dr. Ling Wang and Dr. Shunbin Ning, for their support. I want to thank Dr. Ling Wang for performing the confocal microscopy, and Ms. Xindi Dang for contributing to the topoisomerase II alpha activity assay, T cell dysfunction, and apoptosis experiments used in this study.

I would also like to acknowledge the members of Dr. Yao and Dr. Moorman's lab: Lam Ngoc Thao Nguyen, Lam Nhat Nguyen, Juan Zhao, Dechao Cao, Sushant Khanal, Madison Schank, B.K Chand Thakuri, Zhengke Li, Jingyu Zhang, Zheng D. Morrison, and Xiao Yuan Wu for all their support.

Finally, I am grateful for the love and encouragement from my siblings, Chidi, Emeka, and Chidera, and my best friends, Saheed and Clinton. This would not be possible without their support.

TABLE OF CONTENTS

Page

LIST OF TABLES

Table Page

LIST OF FIGURES

CHAPTER 1

INTRODUCTION

Chronic viral infections pose a major threat to public health. They cause debilitating illnesses associated with increased mortality and morbidity. During my master's thesis, I was interested in understanding the role of topoisomerase 2 alpha (Top2α) in T cell DNA topology, immune dysregulation, and DNA damage during viral infections. $CD4^+$ T cells from chronic hepatitis B virus (HBV), hepatitis C virus (HCV), and human immunodeficiency virus (HIV) infected individuals or treated with Top2a inhibitor or poisoner were the primary model used in this thesis.

Topoisomerases are enzymes that regulate the conformation of the DNA by creating transient breaks and resealing the DNA backbone almost at once. This means that a low level of expression or functional activity of this enzyme will cause some problems in DNA topology. On the other hand, the telomeres are hexameric nucleotide sequences (TTAGGG) that cap the ends of the eukaryotic chromosomes and are fundamental in maintaining genomic integrity. Shortening of the telomeres leads to DNA damage, poor cellular proliferation capability, and T cell dysfunction or apoptosis.

In the introduction, I begin by briefly talking about the virology, epidemiology, and transmission of HBV, HCV, and HIV infections. Then I proceed to discuss an overview of chronic viral infections and T cell dysregulation, chronic viral infections, and telomeric DNA damage. Finally, I conclude by elaborating on the role of topoisomerases and the possibility of topoisomerases inhibition as therapeutic options.

Epidemiology, Virology, and Transmission of Chronic Viral Infections

Hepatitis B Virus (HBV) Infection

The hepatitis epidemic was first recognized in 1883 during a vaccination program in Bremen Germany during which some shipyard workers who were injected with smallpox vaccine became icteric weeks after the vaccination.[1] In the early 1940s, there was another major outbreak of hepatitis which occurred in American Army personnels following a possibly contaminated yellow fever vaccine. [1] However, the idea of its etiology remained mostly unknown until the mid-1960s when an antigen observed in the serum of thalassemia patients transfused with large amounts of blood was noted to be associated with post-transfusion hepatitis.[1–4] This antigen (Australian Antigen) became a serological marker for active hepatitis B virus infection.[1,2] This viral infection became a public health concern only after the laboratory markers of the hepatitis B viral infection (notably the antigen of the hepatitis B virus surface) was observed to have persisted in individuals with a chronic liver infection. [1]

According to World Health Organization (WHO), by the end of 2015, it was estimated that approximately 257 million people were living with chronic hepatitis B virus infection and that this virus resulted in about 887,000 deaths, mainly from primary liver carcinoma. [5]As in 2016, just 10.5 percent of these populations were aware of their infection, and an estimated 4.5 million of the individuals diagnosed were on antiviral therapy. Prevalence of hepatitis B was noted to be highest in the Western Pacific and African region where about 6.2 percent and 6.1 percent of the adults were infected respectively; and lowest in the Eastern Mediterranean, Southeast Asian and European region with 3.3%, 2.0% and 1.6% of the population are affected. [5]

Aaron M. Harris and his colleagues reported that about 2.2 million persons are infected with the hepatitis B virus in the United States, and 15 to 20% of these individuals are likely to die prematurely from hepatic complications and liver cancer. [6]

HBV can be transmitted perinatally, through sexual contact with infected individuals, and parenteral transmission, which can be from intravenous drug use, transfusion of blood and blood products, dialysis, and exposure to infected body fluids such as seminal, vaginal fluids, and saliva.

HBV is a partially double-stranded DNA virus and belongs to the *Hepadnaviridae* viral family. It is an enveloped virus and has an icosahedral capsid. The viral genome comprises four open reading frames (ORFs). The largest ORF known as the P gene, encodes the viral DNA polymerase. The S gene and domain, which is the second-largest ORF encodes the three enveloped proteins named large, middle, and small hepatitis B surface antigen (HbsAg). The C gene known as the core encodes the capsid protein, and finally, the X ORF which is the smallest encodes the 154 amino acid of the X protein known as the HBx protein. The HBx protein is associated with the ability of the virus to replicate and disrupt host cellular responses. Once the virus attaches to a host cell, it becomes uncoated. Inside the cell, the partially double-stranded genome is transported to the nucleus and converted to a covalently closed circular DNA. This covalent closed circular DNA serves as a template for the production of the viral transcripts. [7–10]

Following infection with HBV, there is an initial phase of acute infection in which the affected individual may be asymptomatic or present with nausea, vomiting, increased liver span, and jaundice (yellowness of the eyes, skin, and urine). During this acute phase, the virus can be cleared within six months in 90-95% or may become chronic in about 5-10% in infected adults. This virus targets the liver cells, leading to chronic inflammation of the liver (viral hepatitis).

Hepatitis is a risk factor for liver cancer. Chronic HBV infected individuals express hepatitis B surface antigen (HBsAg) and hepatitis B e antigen (HbeAg) in their serum. HbsAg and HbeAg are used as serological markers for diagnosis. HBV infection is a vaccine-preventable disease with the vaccine having a notable safety profile since it became available in 1982. [5,7,11]

Hepatitis C Virus (HCV) Infection

In 1975, after the progress in the definite diagnosis of hepatitis A virus (HAV) and HBV and identification of other hepatitis inducing agents, Feinstone and his colleagues noticed that most of the post-transfusion associated hepatitis in twenty-two patients were negative for HBV and HAV. [12] In another report, a similar finding was observed in thirty-four cardiac surgery patients who developed hepatitis after blood transfusion postoperatively.[13] This occurrence prompted the need for the identification of this non-A non-B hepatitis (NANBH) agent. It was not until 1989 more than a decade later that Choo and his colleagues isolated a complementary DNA (cDNA) clone derived from the RNA molecule present in the serum of a patient infected with NANBH agent. This NANBH agent was called HCV by this group.[14]

According to the WHO, an estimated 170 million people are infected with chronic HCV infections worldwide; and about 1.2 million individuals died from HCV infections in 2015. These deaths were primarily due to its associated liver complications, notably liver cirrhosis and HCC. [15,16] In America, an estimated 3.5 million people are infected with chronic HCV infection.[16] The prevalence of HCV has skyrocketed in recent years due to the high rate of intravenous drug abuse.

HCV can be transmitted mostly through contact with infected blood and blood products, which may be through intravenous drug use, blood transfusion, unsafe sexual practices, organ transplantation, and perinatally from mother to child during delivery.

HCV is an enveloped, single-stranded linear RNA virus. It has an icosahedral nucleocapsid of about 9.6 kb and belongs to the *Flaviviridae* family. It consists of a single ORF that encodes a single viral polyprotein. This polyprotein is cleaved afterward by viral and host proteases into ten different viral proteins with distinct features namely envelope glycoproteins E1 and E2, core protein, p7 ion channel protein, and finally the NS2, NS3, NS4A, NS4B, NS5A, and NS5B proteins, all of which are non-structural proteins. These proteins promote viral replication, entry, and viral pathogenesis.[17,18]

Once infected with HCV, there is an initial phase of acute infection in which the individual is asymptomatic or may have non-specific clinical signs, such as malaise, anorexia, and abdominal discomfort. Infection tends to resolve in 15 to 20 percent of affected individuals. However, 75 to 80 percent of individuals develop chronic HCV infection.[17] There is currently no vaccine for HCV infection, and attempts aimed at minimizing the burden of HCV infection are geared towards primary and secondary prevention strategies as well as antiviral treatment.

Human Immunodeficiency Virus (HIV) Infection

It was thought that simian immunodeficiency virus (SIV), a virus that infects nonhuman primates such as chimpanzees and sooty mangabey monkeys in sub-Saharan Africa, mutated into HIV in humans after crossing several cross-species barriers; and that hunters in the southeastern part of Cameroon had contact with the blood of these infected animals.[19] Retrospective analysis of the blood samples taken from a man living in Kinshasa in 1959 detected HIV, and this was the first verified case of HIV infection. Kinshasa was a growing place at that time with a thriving sex trade. HIV began to spread into other areas over the decades, and eventually became a global epidemic.[20,21]

According to the WHO, an estimated 37.9 million people are living with HIV as of 2018, with about 1.7 million new infections and 77,700 HIV-related deaths in 2018. In 2018, 23.3 million (62%) of the affected individuals were receiving antiretroviral drugs. HIV can be transmitted through unsafe sexual practices, intravenous drug use, blood and blood products, and perinatally from mother to child.[21,22]

HIV is a single-stranded enveloped positive-sense virus with a complex, conical capsid belonging to the *retroviridae* family of RNA virus, a subgroup of the *Lentivirus.* It has a diploid genome. It encodes three structural genes, namely envelope (that codes for glycoproteins gp120 and gp41), gag gene (that codes p24 and p17, which are capsid and matrix proteins, respectively), and the pol gene (that codes for reverse transcriptase, protease, and integrase). HIV mainly targets T cells and macrophages. The enveloped proteins mediate entry and attachment of the virus to the T cells, and once entered the cytoplasm of the host cell, and the capsid releases the viral RNA. This viral RNA is reverse transcribed into double-stranded DNA (dsDNA) and incorporated into the host genome by an enzyme called integrase. On cellular activation, the viral DNA is continuously transcribed, and new transcripts are produced.[20,23,24]

Before the commencement of antiretroviral therapy (ART), HIV infection progresses through three main phases. There is an initial phase of acute infection characterized by non-specific symptoms such as fever, chills, and headache, and lasts for two to four weeks. This phase is marked by rapid viral replication, dissemination, and seeding into lymphoid tissues. This is followed by clinical latency (chronic HIV infection) whereby viral replication occurs at a very low level. At this point, the infected individuals may be asymptomatic. This phase progresses to AIDS eight to ten years and marked by systemic immunodeficiency, opportunistic infections, AIDS-defining illness, and eventually death without ART. Even though there is not yet a cure for

HIV infection, adequate adherence to ART therapy helps suppress the viral load, and these individuals tend to live longer and healthier lives.

Chronic Viral Infections and T cell Dysregulation

The clearance of these viruses, as well as other pathogenic infections, is mostly dependent upon the activation of T cells by the adaptive immune system. However, by some incompletely understood mechanisms, these T cell responses and adaptive immune responses become depressed and inefficient to clear viral infections. Thus, viral infection-mediated symptoms persist for a long time. Despite this, exposure to these infections contributes to the shaping and development of our immune systems.

Laboratory mice which are known to live in sterile confinements were observed to have less developed immune system evidenced by the lack of $CD8^+$ T cells, a vital arm of the adaptive immune system compared to commercial pet store mice. Furthermore, significant changes to many immune cell lineages were observed on co-housing with commercial pet store mice. Also, Reese and his group reported that vaccine and immune responses were altered in laboratory mice on the persistent exposure to common pathogens compared to their mock mice, confirming possible profound immune boosting with exposure to pathogens.[25] This means that the interaction between the pathogens and host cells determines to a large extent, the balance between disease progression and host immunity.

Chronic viral infections have been shown to cause T cell exhaustion, which is a state of low proliferative potential as a result of continuous antigenic exposure. Proper differentiation of T cells, especially the $CD4^+$ T cells to Th1 subtype, is essential in the control of chronic viral infections. Using *in vivo* labeling techniques, Beura and his group studied the impact of viral persistence on T cell differentiation on mice models. They compared immune responses to

different strains of lymphocytic choriomeningitis virus (LCMV) known to cause acute and chronic infections; and observed that after the first week of infection, there was a marked reduction in the cytokine-producing cells in the mice infected with the LCMV strain of chronic infection compared to the acute infection mice models.[26] This means that a fully functional $CD4^+$ T cell repertoire plays a crucial role in halting viral persistence.

Similarly, studies in humans noted loss in the proliferative ability and functionality of the $CD4^+$ T cells, especially in HIV and HCV infections that lead to chronic viral persistence. This loss in responsiveness has been thought to be a result of poor differentiation of the $CD4^+$ T cells into functional subsets and deficiency in the production of cytokines and co-regulatory molecules. [27–30]

Telomeric DNA Damage and Chronic Viral Infections

Chronic viral infections are characterized by the upregulation of biomarkers of senescence, such as phosphorylated histone H2AX (γ-H2AX), miR-21 and $p16^{INK4A}$, and most importantly telomere shortening.[31–33]

Telomeres are repetitive hexameric nucleotide repeat sequences (TTAGGG) found at the ends of the eukaryotic chromosomes, along with a complex of proteins called shelterin. They are paramount for maintaining genomic integrity and prevent loss and fusion of the chromosomal ends. The shelterin proteins, which includes telomeric repeat-binding protein 1 (TRF1), telomeric repeat-binding protein 2 (TRF2), protection of telomere 1 (POT1), TRF1 and TRF2 interacting nuclear protein 2 (TIN2), TIN2 and POT1 interacting protein 1 (TPP1), TIN2 and POT1 interacting protein 1 (TPP1), and repressor activator protein 1 (RAP1) function together to protect the telomeres. The telomeres shorten during each cell division and the telomerase enzyme

function to replenish the telomere length. Cells with shortened telomeres are recognized as DNA damaged with phenotypic reconditioning that drives cellular apoptosis.

Kim and his group knocked out specific subunits of the shelterin complex in the human cell line using the CRISPR/Cas 9 technology to systematically profile the role of each shelterin protein in maintaining telomere integrity and function. They noted that removal of any subunit of the shelterin complex leads to telomere deprotection, chromosomal fusion, induction of the DNA damage response proteins, such as ataxia -telangiectasia mutated (ATM), and metabolic dysfunction, suggesting a tightly regulated process in telomere assembly.[34]

Nguyen et al. reported that suppression of TRF2 protein expedited telomere attrition, apoptosis, and DNA damage in individuals with chronic HCV infection compared to healthy subjects. [35] Also, there are reports of telomere shortening impairing DNA damage repair and undoubtedly having pathological repercussions.[36–39]

Topoisomerases and Topoisomerase Inhibitors or Poisoners as Therapeutic Options

There is a strong relationship between the DNA structure and the cellular processes that occur in the cells. The DNA is a double-stranded helical structure wound around a core of histone proteins and condensed in a chromatin assembly. While this conformation is essential in maintaining and preserving genetic information, it also poses some form of topological problems. This is because nearly all the cellular processes such as DNA replication, transcription as well as gene recombination involve separation of this double helix in order to access the preserved information in the DNA and could create torsional stress on the DNA structure. This topology could be in the form of supercoils, catenations, and molecular knots and must be resolved for effective physiological functions and efficient gene expression. These constraints

are resolved by DNA topoisomerases, which are enzymes that adjust the DNA topology in the cell. [40]

These topoisomerases make transient single- or double-stranded breaks in the DNA backbone; therefore, allowing the release of this topological stress. At the end of the genetic process, the backbone is ligated immediately. These enzymes are indispensable for the survival of all entities and, thus, common to all cellular structures. There are two main categories of topoisomerases, type I, and type II. While type I topoisomerases resolve DNA entanglements by making a single break in one of the DNA strands, passing the uncleaved DNA strand through the break and finally resealing the backbone, type II topoisomerases make double-stranded breaks through which adjustments in the DNA topology occurs. [41]

Top 2α, a type II topoisomerase, is fundamental for the vitality of rapidly growing cells. Its level rises significantly during G_1 to S and G_2 to M cell cycle progression. Despite being crucial for cell growth and vitality, it tends to fragment the genome. This is as a result of the generation of a phosphotyrosyl bond that covalently links the protein to the 3' – hydroxyl and 5' – terminus of the DNA moiety called Topoisomerase II –DNA cleavage complexes (Top2cc). Interestingly, this Top2cc is transitory, easily reversible, and is paramount for it to perform its genetic function; and thus, their levels must be maintained tightly. Low levels of the Top2cc lead to the poor separation of daughter chromosomes during mitosis, and thus, these cells die from a fatal mitotic breakdown. Also, increased levels of Top2cc lead to the conversion of these transient double-stranded breaks into permanent double-stranded breaks that can overpower the cells and initiate cell apoptosis. [42–44]

Since Top2α is highly expressed in rapidly proliferating cells such as cancer cells, it has been used as a prognostic cancer cell biomarker and a primary target of many anticancer drugs as

well as some antibacterial medications such as fluoroquinolones. These inhibitors act by two recognizable mechanisms: either by inhibiting the catalytic activity of Top2α from completing the ligation of the cleaved DNA molecules or, by increasing the levels of the Top2cc. [41,45–54]While much is known about the role of topoisomerases in cancer and bacterial cells; very little is known on how Top2α level is regulated during chronic viral infections.

Hypothesis

Topoisomerase 2 alpha levels may be disrupted, leading to DNA damage and immune dysregulation in individuals with chronic viral infections.

CHAPTER 2

EXPERIMENTAL PROCEDURES

Ethics Statement

The study protocol was approved by the Institutional review board of East Tennessee State University and James H. Quillen VA Medical Center, Johnson City. All participating adults in this project signed the informed consent form.

Subjects

The study groups consisted of four populations: Chronically HBV-infected individuals on therapy, chronically HCV infected patients, and chronically HIV-infected patients on antiretroviral therapy; and age-matched healthy subjects. Blood samples from healthy subjects were supplied by Physicians Plasma Alliance in Gray, Tennessee, and negative for HIV, HCV, and HBV infection.

Cell Isolation and Culture

Peripheral Blood Mononuclear Cell (PBMC) Isolation

In studying human immune response to diverse stimuli, PBMCs are isolated from whole blood. These cells are composed of a diverse population of cells of varying frequencies; they include monocytes, lymphocytes, dendritic cells, and stem cells.

PBMCs were isolated from the whole blood of the study participants by Ficoll density centrifugation using the Ficoll-Paque plus solution (GE Healthway, Piscataway, NJ; C# GE17-1440-03) and the manufacturer's instructions were followed. In brief, anticoagulant-treated blood diluted with an equal volume of 1x RPMI 1640 with L-glutamine (Corning Mediatech C# 10-040-CV) was layered over 15ml of Ficoll-Paque plus solution in a 50 ml centrifugation tube. Care was taken to prevent the mixing of the solution and the diluted blood sample. The blood

sample was centrifugated at 2000 rpm for 20 minutes at 24 degrees with acceleration and deceleration speeds set at 1. After centrifugation, visible layers were noted and using a sterile pipet, the upper layer containing the plasma was aspirated and was discarded or stored for future use. At the interphase between the plasma and the Ficoll solution lies the PBMCs. They were carefully removed and transferred into another 50 ml conical tube containing three times the volume of RPMI 1640 media and centrifuged at 1800 rpm at room temperature for 8 minutes with acceleration and deceleration speeds set at 9 to remove any remaining Ficoll solution. The cells were counted, and the percentage of live cells estimated by trypan blue staining (1:1 dilution) using the automated cell counter (Invitrogen Countess II FL automated cell counter C# AMQAF1000)

Cryopreservation

Freshly isolated PBMCs are either used immediately or stored for future use in liquid nitrogen. For long term storage, isolated PBMCs were suspended in freezing medium that is 50% RPMI 1640 medium by volume containing 10% dimethyl sulfoxide (DMSO) by volume (Sigma Life Science C# D2660-100ml) and 40% fetal bovine serum (FBS) by volume (Invitrogen Corporation C# 26140-079) and stored at –80 degrees in cryotubes. The next day, they are transferred to the liquid nitrogen tank and stored for future use.

$CD4^+$ T Cell Isolation

$CD4^+$ T cells were isolated from the PBMCs using the human $CD4^+$ T cell negative selection isolation kit (C# 130-096-533) and LS columns from Miltenyl Biotec Inc., Auburn, CA and the manufacturer's cell isolation protocol was followed. Briefly, frozen PBMCs were thawed in a water bath at 37-degree Celsius and transferred to a tube containing the thawing medium of RPMI 1640 to wash the cells. The samples were centrifuged at 900 rpm for 5 minutes. The

supernatant was discarded, and the cells were suspended in 10Ul of biotin- antibody cocktail and 40ul of isolation buffer per 10^7 cells. The suspension was mixed well by slow pipetting and incubated for 5 minutes at 4-degree Celsius. The biotin-antibody cocktail is made up of anti-human biotin-conjugated monoclonal antibodies against CD8a, CD14, CD15, CD19, CD36, CD56, CD123, CD123, TcRγ/δ and CD235a.

Next, 30ul of isolation buffer and 20 ul of $CD4^+$ T cell microbead cocktail was added per 10^7 cells to the suspension, mixed well, and incubated in 4-degree Celsius for 10 minutes and subsequent magnetic cell separation. The flow-through contained the purified CD4 T cells. The cells were counted by trypan blue staining in a counting chamber and utilized for further assays.

Cell Culture

Isolated CD4 T cells were suspended in complete media of RPMI 1640 media containing 10% fetal bovine serum (FBS) (Atlanta Biologicals, Flowery Branch, GA), 100IU/ml of Penicillin and 2mM L-glutamine (Thermo Scientific, Logan, Utah); and seeded into appropriate well plates. Topoisomerase II alpha (Top2α) is only expressed in activated T cells. As such, the cells were stimulated with purified NA/LE mouse anti-human CD3 antibody clone HIT3 α (BD Pharmamingen brand C# 555336) and purified NA/LE mouse anti-human CD 28 antibody clone CD28.2 (BD Pharmingen brand, C#555725) and cultured at 37-degree Celsius and 5% CO_2 atmosphere for 3 days and subsequently used for downstream applications.

RNA Isolation and cDNA Synthesis

Total RNA was isolated from 1x 10^6 CD4 T cells using the RNeasy Mini Kit (Qiagen C# 7410), and the manufacturer's instructions followed accordingly. Cultured cells were harvested and washed with phosphate-buffered saline (Lonza BioWhittaker DPBS, C#17-512F) by centrifuging at 1500rpm for 5 minutes, and the supernatant removed. The pelleted cells were

disrupted and homogenized by the addition of 350uL of Buffer RLT (supplied) per 5 million cells and vortexing for 1 minute. The lysate was centrifugated for 3 minutes at 10000 rpm, and the supernatant was removed by pipetting. One volume of cold 70 percent ethanol was added to the lysate. It was mixed thoroughly by pipetting, and 700uL of the sample was transferred immediately into an RNeasy Mini spin column placed in a 2ml collection tube (supplied). The sample was centrifuged for 15 seconds at 10000rpm, and the flow-through was discarded. 700uL of Buffer RW1 (supplied) was added to the into the spin column followed by brief centrifugation at 10000rpm for 15 seconds and the flow-through discarded. 500ul of Buffer RPE (supplied) was added to the spin column and sample centrifuged at 10000 rpm for 15 seconds with the flow-through discarded. Finally, the spin column was placed in a new 1.5ml collection tube (supplied), and 50ul of RNase free water supplied) was added to the spin column membrane and centrifugated at 10000rpm for 1 minute to elute the RNA. RNA concentrations and quality were determined by photometric analysis (Eppendorf BioPhotometer Model number 6131).

2 ug of RNA per 20uL reaction was reverse transcribed to cDNA using the High Capacity cDNA Reverse transcription Kit (Applied Biosystems C# 4368814) and the manufacturer's instructions followed accordingly. The components of the kit were thawed on ice, and the reverse transcription (RT) master mix was prepared on ice, followed by the manufacturer's recommended volumes for each of the reagents, as shown in Table 1 below. 10uL of RNA sample was added to 10uL of the RT master mix and mixed thoroughly by pipetting. The sample was aliquoted into 0.2mL tubes and spun down to eliminate any air bubbles.

Table 1: Reverse Transcription Master Mix Components

Component	Volume per reaction (uL)
10X RT Buffer	2.0
25X dNTP Mix (100mM)	0.8
10X RT Random primers	2.0
MultiScribe Reverse Transcriptase	1.0
RNase Inhibitor	1.0
Nuclease free water	3.2
Total per reaction	10

The tubes were placed on the thermal cycler (Biorad T100 Thermal Cycler C#1861096) and programmed using the thermal cycler conditions recommended by the manufacturer and listed in Table 2.

Table 2: cDNA Reverse Transcription Thermal Cycler Conditions

	Step 1	Step 2	Step 3	Step 4
Temperature (°C)	25	37	85	4
Time (minutes)	10	120	5	∞

Quantitative Real-time Reverse Transcriptase PCR Analysis (RT-PCR)

The cDNA synthesized from the reverse transcription reaction was incubated with a 10uL SYBR Green master mix (Biorad, USA iTaq Universal SYBR Green one-step kit C#1725150), 8uL of distilled filtered water, 1 uL of forward and reverse primer per 20uL reaction. The

primers used were purchased from Thermo Fisher, and primer concentrations were optimized to a final concentration of 5uM/uL. GAPDH was used as the loading control, and gene expression was determined using the $2^{-\Delta\Delta ct}$ method. The list of primer sequences used are shown in table 3 below

Table 3: List of PCR primers used in this study.

Primers	Forward sequence	Reverse sequence
Top 2α	5′-ACCATTGCAGCCTGTAAATGA-3’	5′-GGGCGGAGCAAAATATGTTCC-3’
hTERT	5′-CCAAGTTCCTGCACTGGCTGA-3′	5′-TTCCCGATGCTGCCTGACC-3′
GAPDH	5′-TGCACCACCAACTGCTTAGC-3′	5′-GGCATGGACTGTGGTCATGAG-3′

Protein Extraction and Western Blotting

$CD4^+$ T cells were harvested and washed with 500uL of iced cold isolation buffer by centrifuging at 1500rpm for 5 minutes. The supernatant was decanted, and the cells were suspended in RIPA buffer (Boston BioProducts, C# BP-407) with a 1x pierce protease inhibitor tablet (Thermo Scientific, C# A32953). The samples were mixed thoroughly by vortexing for 15s, and the contents were incubated for 30 minutes at 2-degree Celsius on a rocking platform. The lysates were centrifugated for 15 minutes at 13200rpm, and the supernatant containing the purified protein was transferred into a 1.5mL tube and kept on ice. Protein concentration was determined by the Bradford protein concentration assay, and a 4x SDS loading buffer was added to the lysates. The lysates were heated for 5 minutes at 95-degree Celsius to denature the proteins. Following SDS-PAGE gel electrophoresis, the proteins were transferred onto a PVDF membrane in an overnight wet transfer. The membranes were blocked with 5% skim milk in 1x tris-buffered saline containing 0.1% tween (TBST) for 1 hour at room temperature on a rocking

platform; thereafter, they were washed with 1x TBST thrice and probed with specific primary antibodies (in 1x BSA solution) and secondary antibodies (in 5% skim milk). Primary antibodies included Top2α, PARP1, Caspase 3, gamma γH2AX, TRF2, TRF1, TIN2, RAP1, POT1, β-actin, ATM, and CHK2; secondary antibodies included horseradish peroxide conjugated anti-mouse/anti-rabbit IgG antibodies (Cell Signalling). Chemiluminescence signal was detected by the Biorad Chemi Doc^{TM} MP Imaging system, and western blot images were analyzed with the image lab software (Biorad).

Flow Cytometry (FCM)

Cytokine production, gamma H2AX levels (a DNA damage marker), Annexin V/7-Amino Actinomycin D(7-AAD) assay for cell apoptosis determination and telomere length estimation were analyzed by flow cytometry.

Intracellular Cytokine Staining

Cytokine production and secretion is a key determinant of the strength of cellular immune response. Cytokines are involved in numerous immune responses, including but not limited to activation of T cell proliferation by interleukin-2 (IL-2) and induction of anti-viral proteins by interferon-gamma (INF-gamma); thus, intracellular staining of INF-gamma and IL-2 was analyzed to determine antigen-specific response.

Briefly, 5 million $CD4^+$ T cells were stimulated with CD3/CD28 antibodies, treated with DMSO (control) or etoposide (a Top2a inhibitor), and cultured in a 48 well plate for three days. Brefeldin A (a protein transport inhibitor) and ionomycin were added to the samples 6 hours before harvesting the cells. The cells were washed with isolation buffer by centrifugation for 5 minutes at 1500 rpm, and the supernatant was discarded. The pellets were suspended in 100uL of fixation buffer (Biolegend, C#420801) and incubated in the dark for 40 minutes. The lysates

were centrifugated at 1500 rpm for 5 minutes and the supernatant discarded. The fixed cells are suspended in a 1x permeabilization buffer and centrifugated at 1500 rpm for 5 minutes, and the supernatant removed. The cells pellets were resuspended in 50uL of 1x permeabilization buffer, and 1uL of fluorescence -conjugated antibody of interest was added to the fixed cells for 45 minutes. The fixed and intracellularly labeled cells were resuspended in 50uL of cell staining buffer alongside appropriate controls (unstained, IL-2 only and INF- gamma only) and analyzed by FCM

Annexin V/ 7-AAD Staining Assay

Apoptosis of cells was determined by staining with Annexin V and 7-AAD solutions. This assay is based on the principle that cells undergoing apoptosis flip their membrane by the action of scramblases and phosphatidylserine, a normally intracytoplasmic phosphoprotein is exposed to the outer plasma membrane and this can be bound tightly by annexin V. Also, these apoptotic cells have permeable membranes allowing the leakage of DNA contents and 7-AAD, a DNA binding dye can adhere to the double-stranded DNA and exclude dead cells.
Briefly, 1 million CD4 T cells were stimulated with CD3/CD28 antibodies, treated with DMSO (control) or etoposide (a Top2α inhibitor), and cultured in a 48 well plate for three days. The cells were harvested and washed once with ice-cold PBS and once by 1x binding buffer by centrifugation at 1500rpm for 5 minutes, and the supernatant was removed. The cell pellets were resuspended in 1x binding buffer at 1 million cells/mL, and 100uL of the cell suspension was transferred to a 1.5mL tube. 5uL of fluorescently labeled Annexin V (BioLegend, C# 640922) was added to the samples and incubated for 10 minutes in a dark room and subsequently centrifugated at 1500 rpm for five minutes. The supernatant was removed, and cells resuspended in 100uL 1x binding buffer and incubated with 5uL of 7-AAD staining solution (BioLegend, C#

640922) for 15 minutes away from light. 400uL of 1x binding buffer was added, and the sample analyzed by FCM.

Fluorescent In- Situ Hybridization (Flow-FISH)

The flow-fish technique uses fluorescently labeled nucleic acid probes that bind repetitive sequences at specific sites of the chromosome; and as such, has been used to measure telomere length. Briefly, PBMCs were isolated, stained with Alexa Flour 647 anti-human CD4 antibody (CD4-A647) per 1 million cells in a 100uL staining buffer and fixed with cell fixation buffer (BioLegend, C#420801) for 30 minutes at room temperature. After fixation, cell samples were centrifugated and supernatant decanted. The cells were resuspended in 100uL of hybridization buffer and incubated with 1uL of telomere PNA probe (PNA Bio, C#F1009) at a concentration of 0.3ug probe/mL for 15 minutes at room temperature. The samples were placed in the 82-degree fridge for 10 minutes and then overnight at room temperature. The next day, the cells were washed with post hybridization buffer twice and centrifuged at 2400rpm for 7 minutes, and the supernatant removed. The cells were resuspended in isolation buffer and analyzed by FCM

γ-H2AX Staining for Apoptosis

DMSO (control) or Top2a inhibitor-treated cultured cells were harvested and washed was with isolation buffer, centrifugated, and the supernatant removed. The cells were fixed in a 1:1 dilution ratio and incubated for 15 minutes in a dark cupboard at room temperature. Subsequently, the cells were washed with 800ul of isolation buffer, and the supernatant removed. The cells were resuspended in a FoxP3 fixation/permeabilization staining buffer (eBioscience™, C# 00-5523-00) in a ratio of 1:3 (concentrate/diluent) and incubated for 45 minutes in a dark cupboard. The cells were washed isolation buffer and resuspended in 50uL of 1x permeabilization buffer made by diluting a 10x permeabilization buffer (eBioscience™, C# 00-

5523-00). 1uL of fluorescently labeled H2A.X antibody (BioLegend, C# 613404) was added to the cells and incubated for 40 minutes at room temperature away from light. The samples were washed with isolation buffer and resuspended in isolation buffer for analysis by FCM.

Confocal Microscopy

Following DNA damage, there is a recruitment of p53-binding protein 1(53BP1) to the damaged site. 53BP1 serves as a docking platform for the recruitment of the DNA damage repair proteins. In telomeric DNA damage, the interaction between 53BP1 and TRF1(one of the proteins in the shelterin complex) forms a DNA damage focus called telomeric dysfunction-induced foci (TIF). TIFs recognized by the co-localization of TRF1 and 53BP1 serve as a marker of telomeric DNA and are easily detected by confocal microscopy combined with immunofluorescent staining.

$CD4^+$ T cells were stimulated with CD3/CD28 antibodies and cultured for three days. The cells were harvested and washed briefly with isolation buffer. Cells were fixed with 2% paraformaldehyde for 20 minutes, followed by permeabilization with 0.3% Triton X 100 in 1X phosphate-buffered saline solution (PBS) for 10 minutes. After blocking the samples with 5% fetal bovine serum for 1 hour, they were incubated with rabbit anti-53BP1(Cell Signalling) and mouse anti-TRF1(Thermo Fisher) primary antibodies overnight at 4 degrees.

After incubation, the samples were washed with 1X PBS three times and stained with fluorescence-labeled secondary antibodies anti-rabbit IgG-Alexa Flour 488 and anti-mouse IgG-Alexa Flour 555(Invitrogen) in the dark for 1 hour. The cells were washed with 1X PBS, and for nuclear staining, the samples were treated with DAP1 Flouromount-G (SouthernBiotech, Birmingham, AL) Fluorescence images were acquired using a confocal laser-scanning inverted microscope (Leica Confocal, Model TCS sp8, Germany)

Topoisomerase IIα Activity Assay

Top2α activity was quantified by Topoisomerase II Assay Kit -plasmid-based (TopoGen, Inc. Florida USA, C#TG1001-1), and the manufacturer's instructions were followed. In brief, Cell extracts isolated from purified $CD4^+$ T cells were incubated with plasmid DNA substrate and 5X complete reaction buffer (supplied) for 30 minutes at 37 degrees. 4uL of 5x stop buffer was added to the mixture, and samples were loaded onto 1% ethidium containing -agarose gel with marker DNA loading dye and run at 120V for 30 minutes. Gels were destained in water for 15 minutes before imaging with a UV transilluminator (Biorad Chemi Doc™ MP Imaging system). The intensity of the supercoiled DNA was analyzed by gel densitometry.

Statistical Analysis

GraphPad Prism 7 software was used to analyze the data and are presented as mean ± SEM or median with interquartile range. Unpaired Student's t-test or paired T-test was used to compare the differences between two groups. Multiple groups were analyzed by one-way ANOVA with Tukey's HSD multiple comparison test or non-parametric Mann-Whitney U test. P values less than 0.05 were considered statistically significant.

.

Experimental Design

The workflow of the study is shown in Figure 1. Firstly, PBMCs were isolated from the whole blood of chronically HIV-, HCV-, HBV- infected subjects and healthy subjects by Ficoll density centrifugation. From the PBMCs, $CD4^+$ T cells were purified by negative selection using the T cell isolation kit. The cells were stimulated with anti-human CD3/CD4 antibodies and cultured in an RPMI-containing medium. The mRNA level of Top2α and other genes of interest was determined by RT-PCR. Next, the protein expression of Top2α, the shelterin proteins, and the DNA damage associated proteins were determined by Western blotting. Subsequently, the effect of Top2α inhibition on T cell function and cellular apoptosis was evaluated by flow cytometry. The telomere length was detected by flow-FISH. And finally, immunofluorescence staining combined with confocal microscopy was used to ascertain if Top2α mediated DNA damage extended to the telomeres.

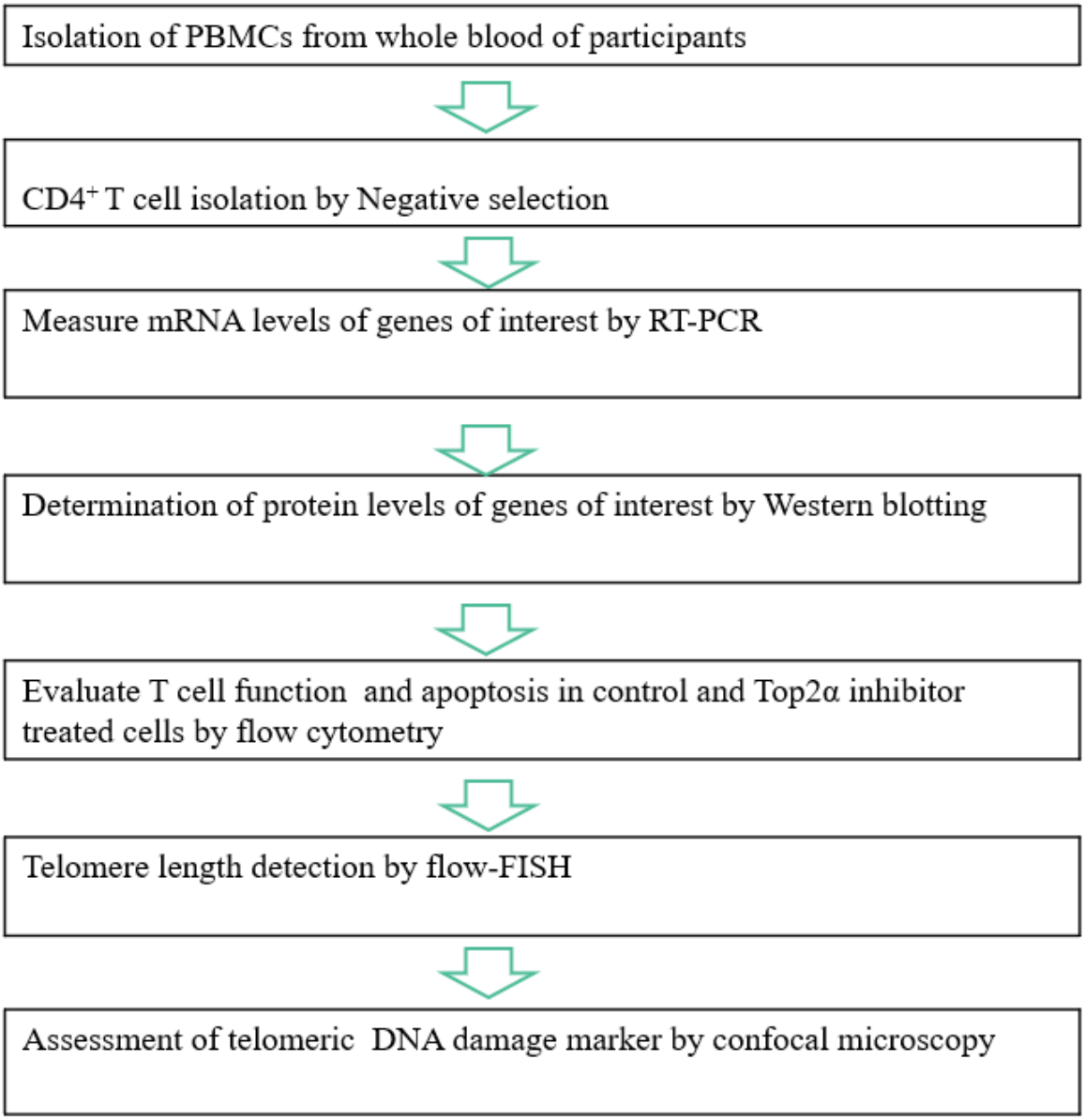

Figure 1: The flow of experimental procedures

CHAPTER 3

RESULTS

Top2α Protein Level is Inhibited during Chronic Viral Infections

The mechanism by which chronic viral (HBV, HCV, HIV) infections alter T cell responses and cause cellular senescence remains poorly understood. Since Top2α is essential in resolving topological problems in the DNA, we hypothesized that its level might be altered during chronic viral infections.

Top2α is only expressed in activated T cells. We examined Top2α protein levels in anti-CD3/CD28-activated $CD4^+$ T cells obtained from chronically HIV-, HCV-, and HBV-infected individuals and compared to healthy subjects by Western blot. As shown in Fig. 2, Top2α level was significantly lowered in $CD4^+$ T cells obtained from the chronically virus-infected patients compared to healthy subjects. The next step was to determine the point at which the inhibition occurred. Top2α mRNA levels were measured in $CD4^+$ T cells from the same subjects by real-time qPCR. As shown in Fig. 3, there was no statistical difference observed at the gene level between the healthy and the virus-infected individuals. These data suggest that Top2α expression level is primarily inhibited at the protein level.

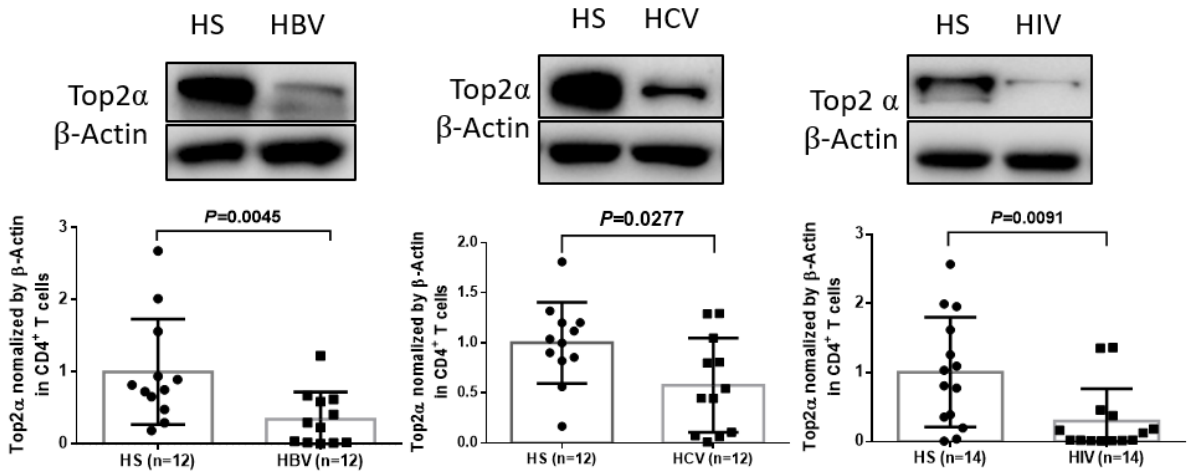

Figure 2: Top2α protein expression between healthy and chronically HBV-, HCV-, and HIV-infected individuals. Summary data and representative blot image are shown. β-actin was used as the loading control. Data were analyzed by using unpaired T-test and reported as mean±SEM, and n represents the number of subjects tested.

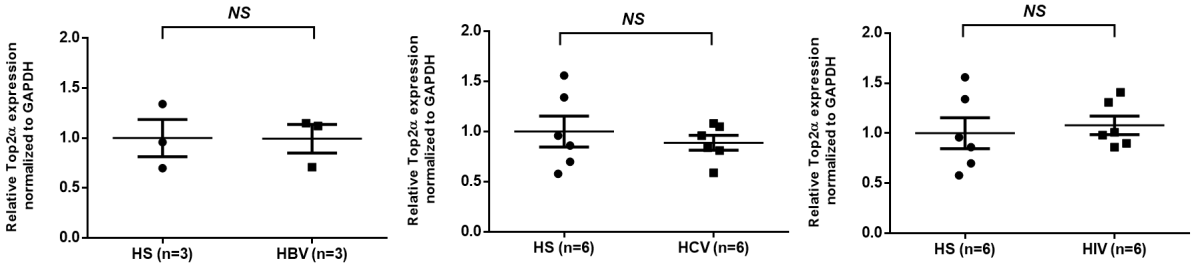

Figure 3: Top2α gene expression between healthy and chronically HBV-, HCV-, and HIV-infected individuals determined by real-time RT-PCR. GAPDH was used as the loading control. Data were analyzed by using unpaired T-test and reported as mean ± SEM, and n represents the number of subjects tested.

Top2α Activity is Suppressed during Chronic Viral Infections

Top2α is a type IIA topoisomerase nuclear enzyme that relieves topological stress in DNA in an ATP dependent process. It does this by creating double-stranded breaks in the

phosphate backbone of the DNA and reseals this almost immediately. By so doing, it relaxes the DNA, allowing effective gene function. Top2α activity level correlates with how well it can relax supercoiled DNA and decatenate kinetoplast DNA (kDNA). Thus, we employed a plasmid-based kDNA Top2α assay kit (Topogen Inc.) to evaluate Top2α activity between healthy and virus-infected individuals.

Catenated kDNA is a large cluster of interwoven DNAs that does not enter the 1 % agarose gel due to its size. Incubation with Top2α effectively decatenates the kDNA into 2.5kb monomeric minicircles (open or closed circular rings) that migrate swiftly into the gel. Top2α activity was compared between HS and individuals with chronic viral infections. As shown in Fig. 4, the linearized kDNA (lane 1) and decatenated kDNA (lane 2) were used as positive controls, extracts from non-stimulated healthy subjects was used as negative control (lane 3), kDNA treated with nuclear extracts from stimulated healthy (lane4), HBV (lane 5), HCV (lane 6), HIV (lane7) subjects resulted in differing degree of decatenation products in the gel. Since Top2α is only expressed in TCR-stimulated cells, it is not surprising that no decatenated DNA topisomers were observed in the gel as Top2α was not expressed. The topological stress was not resolved, and thus, the large catenated kDNA failed to enter the agarose gel. Interestingly, DNA extracts from stimulated HBV-, HCV-, and HIV-infected subjects were unable to decatenate the kDNA effectively when compared to HS. From this experiment, we can conclude that Top2α protein level is directly correlated to its activity.

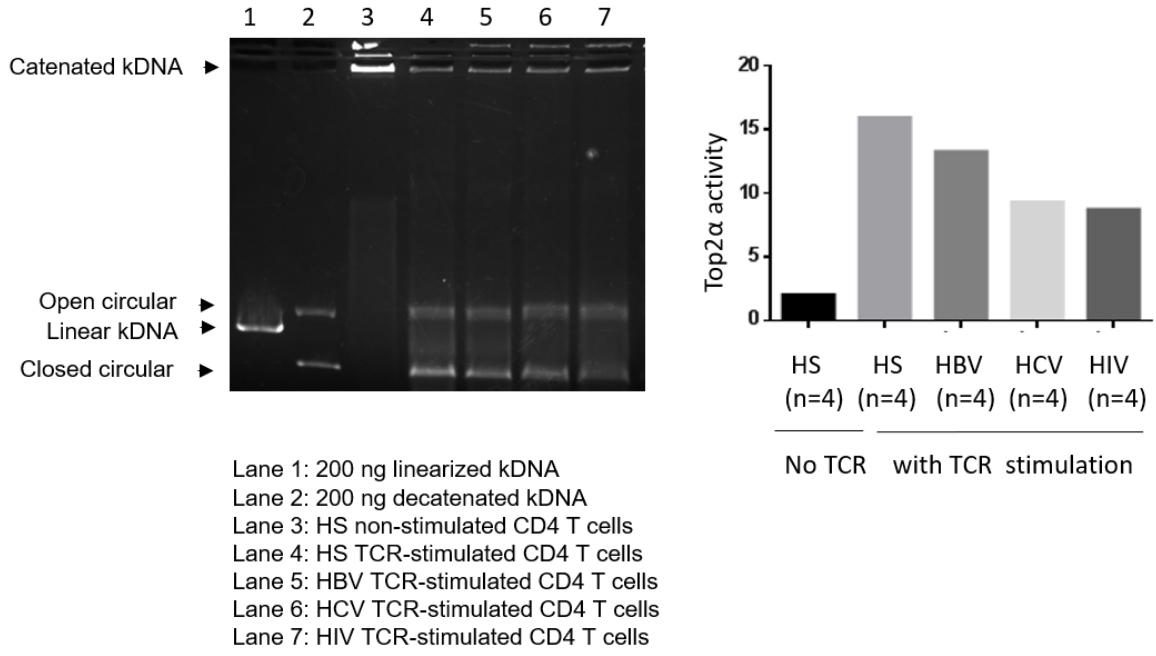

Figure 4: Top2α activity between healthy and chronically HBV-, HCV-, and HIV-infected individuals. Summary data and representative imaging of Top2α cleavage assay. The bar chart represents the relative levels of closed circular monomeric topoisomers from four independent samples, and n represents the number of subjects tested.

Top2α Inhibition Induces T Cell Dysfunction

Top2α is a well-characterized biological target owing to its indispensable role in modifying topological constraints during cell survival and replication. As such, its inhibitor has played an essential role as cancer therapeutics and antibacterial agents. In exploring the role of Top2α inhibition on T cell function, Top2α inhibitor-treated cells were used as models. Etoposide (ETP) and ICRF -193 are topoisomerase II inhibitors or poisoners, and they exert their actions by inhibiting the catalytic activity of Top2α, and in so doing, could convert the transient double-stranded breaks into permanent breaks, thereby damaging the genome. TCR-stimulated $CD4^+$ T

cells derived from healthy subjects were treated with DMSO (control cells) or ETP or ICRF193 (Top2α inhibitor-treated cells) at different time points (6h, 24h, 48h, and 72h) and Top2α expression was observed. As shown in fig. 5a and 5b below, Top2α expression was noticed by 48h post culture, and stronger levels were seen by 72h after TCR stimulation in ICRF193 treated cells.

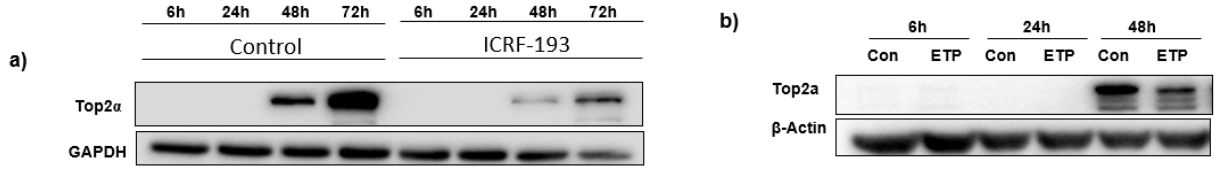

Figure 5. Time-dependent expression of Top2α in TCR-stimulated, inhibitor-treated cells

a) Representative Western blot image of Top2α expression in $CD4^+$ T cells treated with 2ug/ml of ICRF193 at 6h, 24h, 48h, and 72h after TCR stimulation. GAPDH served as the loading control. **b)** Representative Western blot image of Top2α expression in $CD4^+$ T cells treated with 0.2 uM of ETP at 6h, 24h, and 48h after TCR stimulation. β-actin was used as the loading control.

To determine the impact of Top2α inhibition on T cell function, cytokine production was accessed in TCR-stimulated cells exposed to varying concentrations of ETP ranging from 0 uM to 1.0 uM after cell culture for three days by flow cytometry. Cytokine production and secretion are the hallmarks of a functioning T lymphocyte. Production of interleukin -2 (IL-2) and interferon-gamma (INF-γ) was compared in ETP-treated cells versus DMSO control cells. As shown in Fig. 6a, the percentage of IL-2 and INF-γ production were significantly inhibited in ETP-treated TCR-stimulated cells compared to DMSO control. Based on this observation, a concentration was selected and shown in a flow cytometry dot blot in Fig. 6b.

a

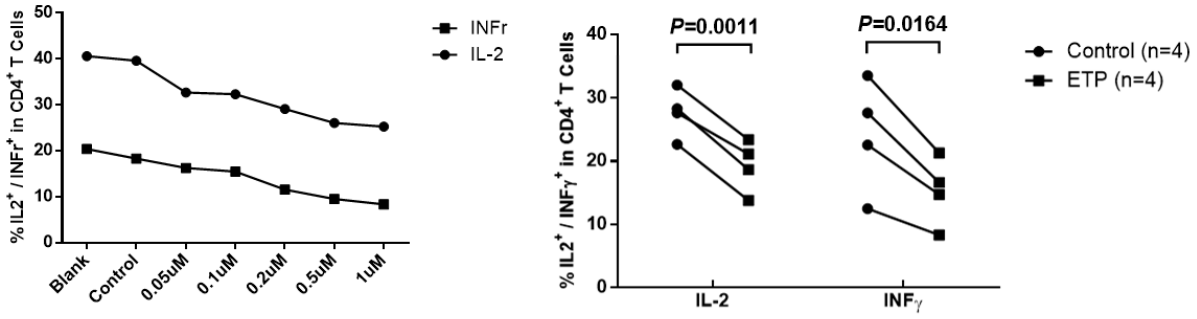

b

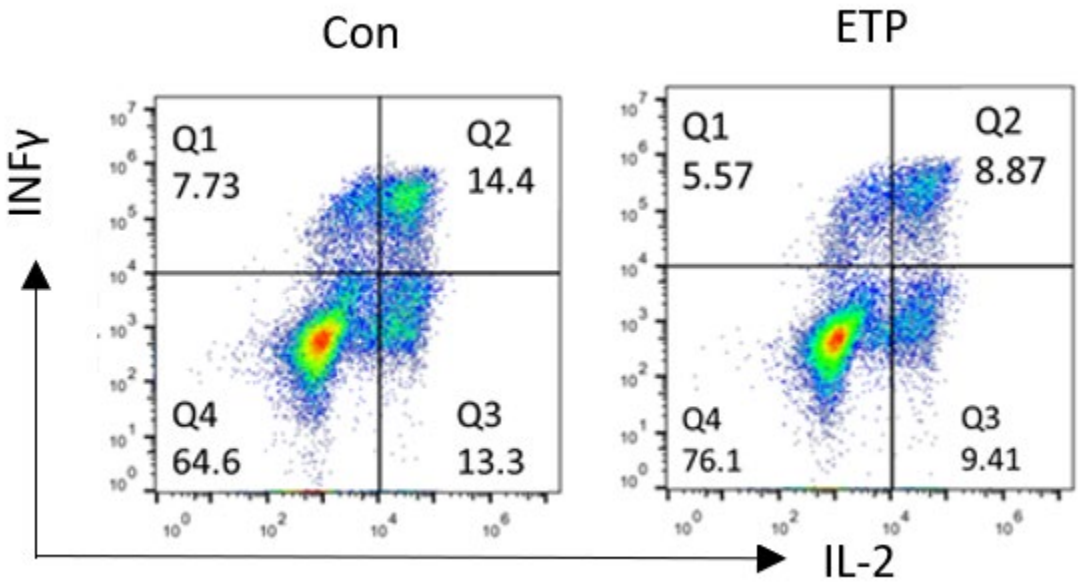

Figure 6. Impact of Top2α inhibition on cytokine production in CD4$^+$ T cells derived from healthy subjects. a) dose-dependent effect of Top2α inhibition on IL-2 and INF-γ production in CD4$^+$ T cells treated with DMSO control or etoposide. Distinct observations from 4 samples recorded and data analyzed by using paired – tests. **b)** Representative flow cytometry dot plot image showing comparisons of IL-2 and INF-γ production between DMSO control and ETP-treated cells.

The next step was to assess the proliferative potential of $CD4^+$ T cells derived from HS under varying conditions (unstimulated, DMSO control, and ICRF193 treated) after three days. Using CFSE dilution tracking dye, cell division, and proliferation was evaluated in T cells. As shown in Fig. 7, T cell proliferation was markedly inhibited in TCR-stimulated, ICRF-193-treated cells compared and to DSMO control, evidenced by the decreased number of proliferation cycles (denoted by the number of peaks). CFSE-labeled cells with no anti-CD3/CD28 stimulation were used as control.

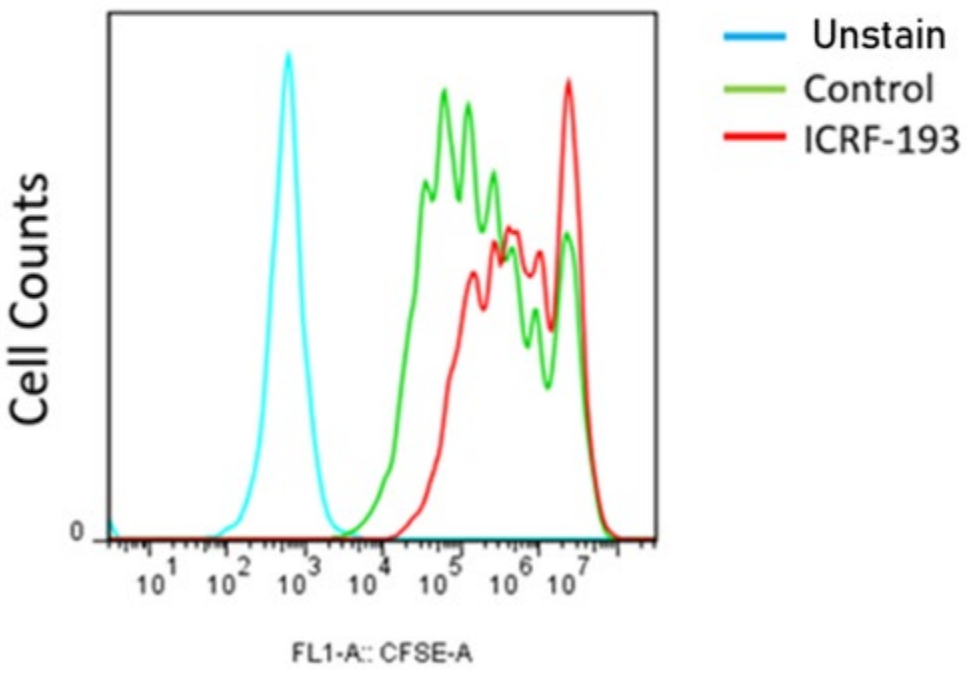

Figure 7. Impact of Top2α inhibition on T cell proliferation determined by flow cytometry

Representative histogram of CFSE dilution comparisons in DMSO control (green histogram) and ICRF-193-treated (red histogram) TCR-stimulated cells after a 3-day culture in $CD4^+$ T cells derived from healthy subjects. Distinct peaks represent cell generation cycles. Overlaid histogram plot was generated by the FlowJo software.

Top2α Inhibition Induces T cell Apoptosis and Boosts Cleaved Caspase 3 Expression

Since Top2α cuts and reseals double-stranded breaks (DSBs) in the DNA backbone, inhibition of its activity may lead to failure of rapidly resealing the backbone and as such, converts these transient breaks into permanent DSBs. We hypothesized that inhibition of Top2α expression and activity might drive these cells to DSB-mediated apoptosis. To this end, we measured apoptosis in TCR-stimulated cells exposed to varying concentrations of ICRF193 (0, 2, 4, and 8μg/ml) at different time points (day 0, 1, 2, 3, and 5) using Annexin V (Av) and 7-Aminoactinomycin D (7-AAD) staining as an indirect measure of membrane asymmetric changes that occur during apoptosis. As shown in Fig. 8, ICRF-193-treated cells exhibited a time- and dose-dependent increases in Av and 7-AAD staining compared to DMSO control.

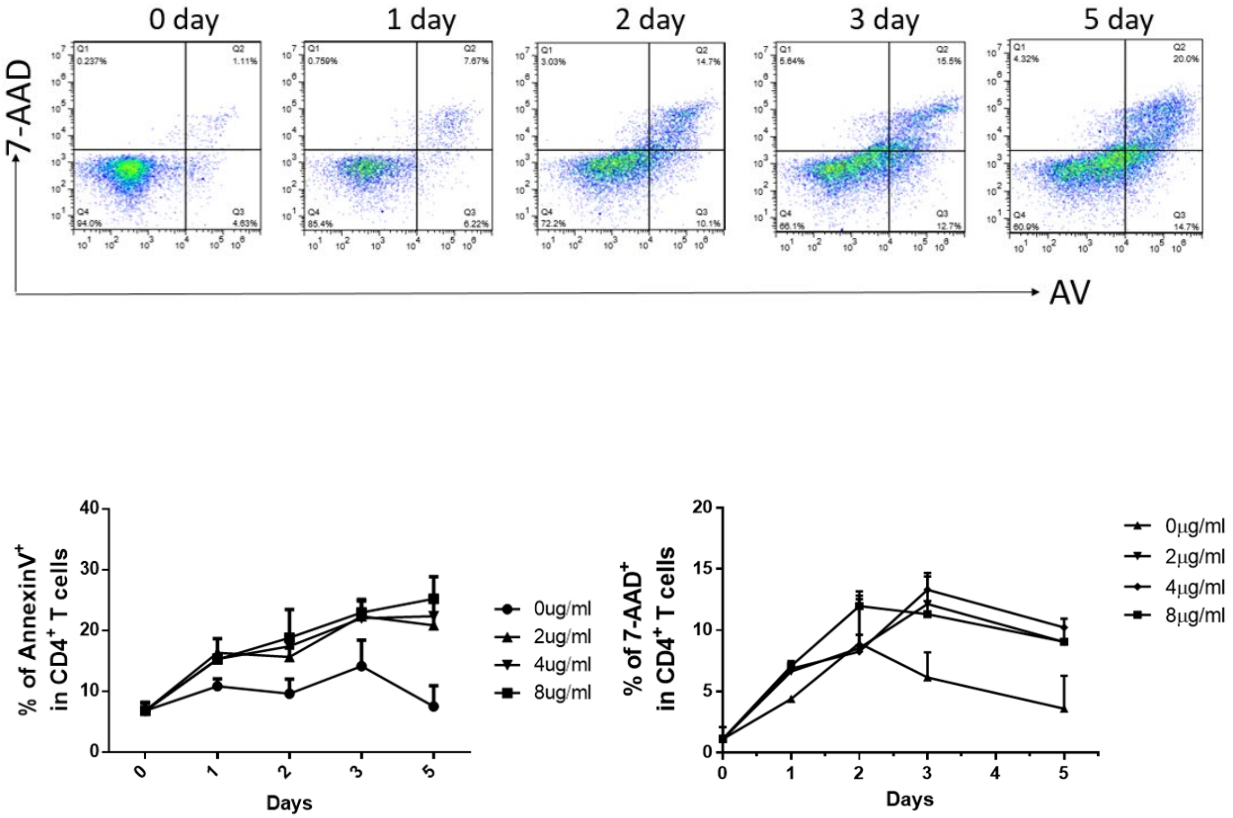

Figure 8. Time- and dose-dependent increases in apoptosis in TCR-stimulated CD4$^+$ T cells by flow cytometry. Representative dot plot image showing the time-dependent increase in Av and 7-AAD staining in TCR-stimulated ICRF-193-treated cells compared to the DMSO control at different time points (0, 1, 2, 3, and 5 days). Dot plots were generated by FlowJo software.

To further validate the apoptosis data, cleaved caspase-3 expression was checked in ICFR-193-treated cells by Western blotting. As shown in Fig. 9, there was a significant upregulation of cleaved caspase-3 in ICRF-193-treated CD4$^+$ T cells compared to the control group.

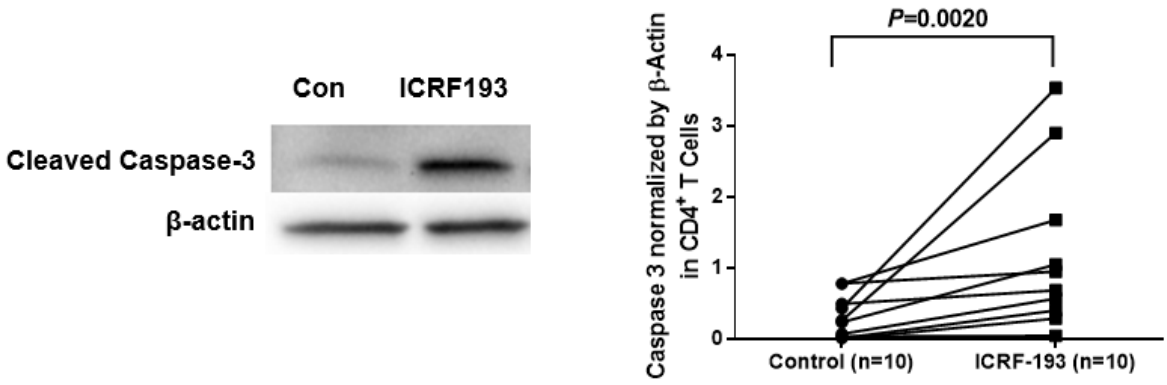

Figure 9. Effect of Top2α inhibition on Caspase-3 expression. Representative western blot image of cleaved caspase-3 expression in DMSO control versus ICRF-193 treated cells. β-actin was used as the loading control. Protein band intensity analyzed with ImageJ software. Summary data of cleaved caspase-3 expression generated by GraphPad Prism software are shown. Data analyzed by paired T-test, and n represents the number of subjects.

Top2α Inhibition Induces Telomeric DNA Damage and Upregulates PARP1 Expression

Since Top2α controls a plethora of gene activity by regulating the winding of the DNA double helix, we hypothesized that Top2α inhibition might induce a DNA damage response as a way to trigger T cell dysfunction. To this end, we measured γ- H2AX, a DNA damage response marker in ICRF-193-treated $CD4^+$ T cells, and compared to DMSO control by flow cytometry. The samples were cultured for three days with anti-CD3/CD28 antibody stimulation. As shown in fig. 10, ICRF-193-treated $CD4^+$ T cells exhibited a significant increase in expression of γ-H2AX compared to DMSO control.

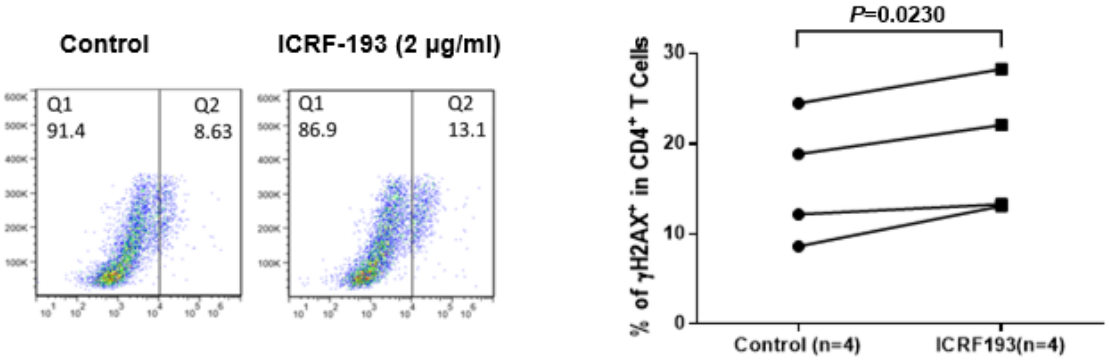

Figure 10. Effect of Top2α inhibition on DNA damage response shown by flow cytometry

Representative dot plot image showing significant activation of the DNA damage response marker, γ- H2AX in TCR-stimulated ICRF-193-treated $CD4^+$ T cells compared to DMSO control after a 3-day culture. Dot plots generated by ImageJ software. Data were analyzed by paired T-test on the GraphPad prism software, and n represents the number of subjects.

To ascertain that the topological DNA damage caused by Top2α inhibition extends to the telomeres, we visualized the dysfunctional telomere-induced foci (TIFs, a marker of telomeric DNA damage) by confocal microscopy following immunofluorescent staining. As shown in fig. 11, the number of TIF per nucleus was significantly elevated in ICRF-193 and ETP-treated cells compared to DMSO control. Taken together, this data confirms our hypothesis that the topological DNA damage caused by Top2α inhibition extends to the telomeres.

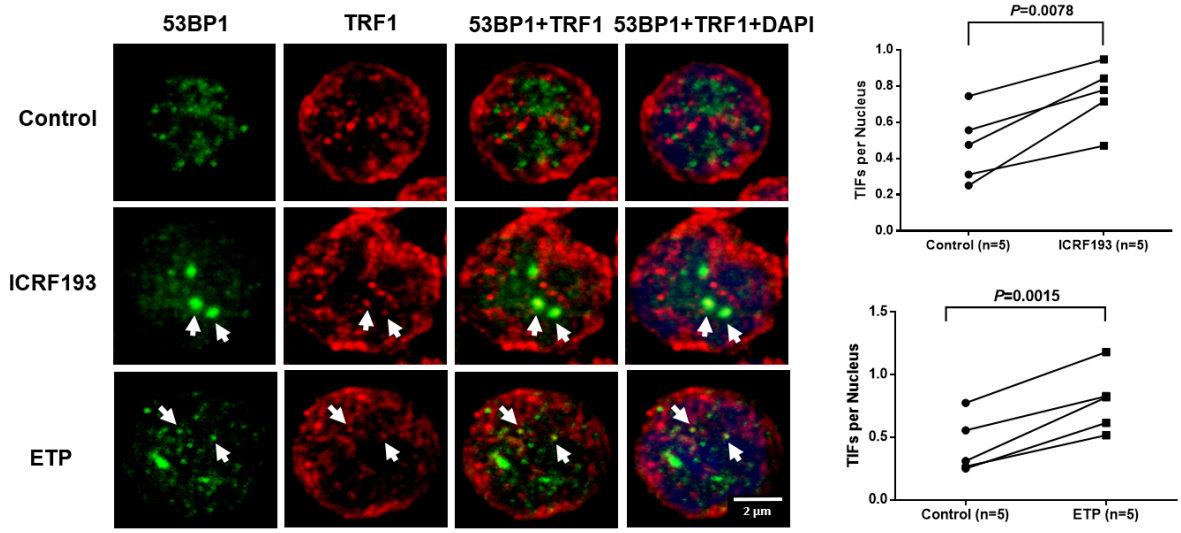

Figure 11: Effect of Top2α inhibition on telomeric DNA by confocal microscopy

Immunocytochemical staining of 53BP1(green) and TRF1(red). Dysfunctional telomere-induced foci per nucleus are identified by the foci that co-stained with TRF1 and 53BP1. The nuclei were stained with DAP1 (blue). Scale bar, 2 µm. Summary data of TIF per nucleus in TCR-stimulated $CD4^+$ T cells exposed to ICRF-193, and ETP versus DMSO control. Data were analyzed by paired T-test on the GraphPad prism software, n represents the number of subjects tested.

Top2α eliminates topological DNA constraints by creating topoisomerase 2 cleavage complexes (Top2cc), a crucial protein-DNA transient intermediate. Any alteration in Top2α activity can lead to the trapping of this Top2cc, causing DNA double-stranded breaks. Repair of Top2α induced DNA break is initiated by tyrosyl-DNA phosphodiesterase 2(TDP2) which catalysis the hydrolysis of the cleavage complexes; and requires the activation poly (ADP-ribose) polymerase (PARP). PARP acts as a DNA break sensor and parylates the target protein by catalyzing the transfer of ADP-ribose. To ascertain if Top2α-mediated DNA damage in T cells involves the cleavage of PARP1, we measured PARP1 expression in TCR-stimulated, Top2α-inhibited cells,

and DMSO control cells after three-day culture. As shown in fig. 12, significant upregulation of cleaved PARP1 was observed in the ICRF193-treated cells.

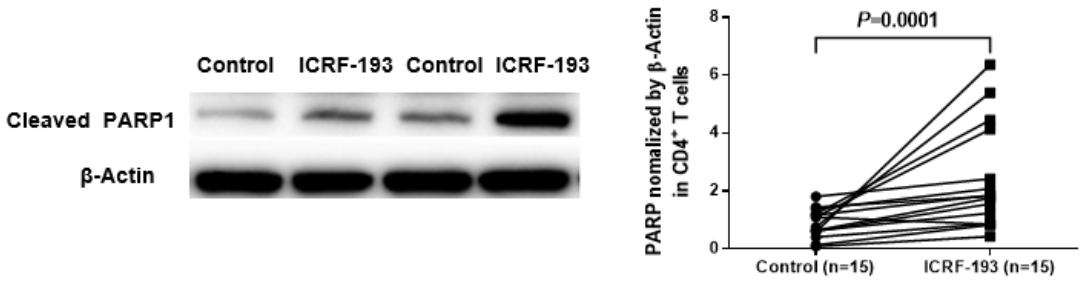

Figure 12. Effect of Top2α inhibition on DNA damage repair protein. Representative western blot image and summary data of cleaved PARP1 expression are shown. β-actin was used as the loading control. Protein band intensity was analyzed with ImageJ software. Summary data of PARP1 expression was generated by GraphPad Prism software. Data were analyzed by paired T-test, n represents the number of subjects tested.

Top2α Inhibition Induces Telomere Shortening by Disrupting the Integrity of the Shelterin Complex and Suppressing Telomerase Activity

Chronic viral infections can cause telomere shortening. The outcome of telomere attrition is premature aging, T cell dysregulation, and immune senescence. To determine if Top2α inhibition leads to telomere attrition, we measured telomere length in TCR-stimulated, Top2α –inhibited cells and compared this to DMSO control after a five-day culture. As seen in fig. 13, there was a significant reduction in telomere length in Top2α-inhibited cells compared to DMSO control. This finding suggests that topological constraints can lead to telomere shortening, similar to what was observed during chronic viral infections.

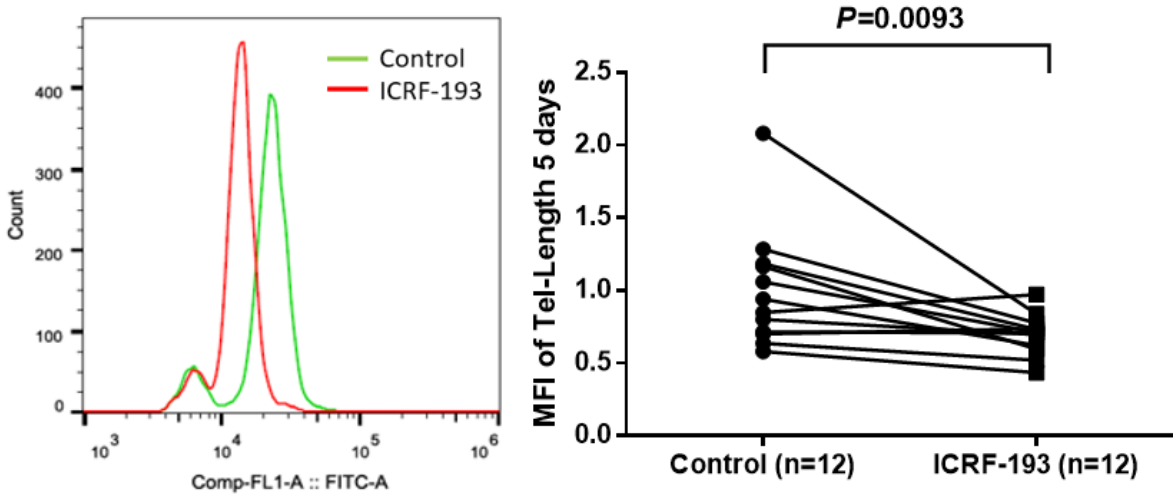

Figure 13: Effect of Top2α inhibition on telomere length measured by Flow-FISH

Representative histogram image showing significant reduction telomere length in TCR-stimulated, ICRF-193-treated $CD4^+$ T cells compared to DMSO control after a 5-day culture. The histogram was generated by ImageJ software. Data were analyzed by paired T-test on the GraphPad prism software, n represents the number of subjects tested.

The shelterin complex is a group of proteins that protects the ends of the linear chromosomes from DNA damage. It consists of six proteins, namely TRF1, TRF2, RAP1, TPP1, POT1, and TIN2. To this end, we explored the integrity of the shelterin complex in Top2α-inhibited cells, as shown in fig. 14, among the proteins examined, only TRF2 expression was significantly decreased. Even though TRF1 expression was decreased, it was not statistically significant. The expression levels of RAP1, POT1, and TPP1 were unchanged. These findings reiterate the results observed in primary $CD4^+$ T cells derived from HCV-infected subjects. [33,35]

TRF2 is the essential protein that protects the chromosomal ends. It does this by preserving the appropriate structure at the telomere ends and prevents the end-to-end fusion of the telomere

termini and allows the recruitment of telomerase to the ends of the linear chromosomes. Its inhibition may lead to the inability of telomerase to access the telomeres.

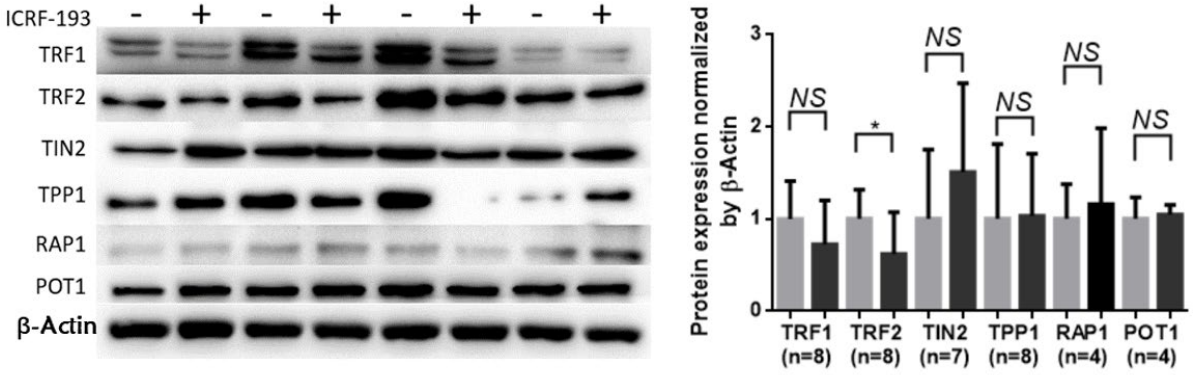

Figure 14: Effect Top2α inhibition on the integrity of the shelterin complex. Representative western blot image and summary data of the proteins in the shelterin complex. Statistically significant inhibition of TRF2 expression was observed. β-actin was used as the loading control. Protein band intensity was analyzed with ImageJ software. Summary data of expression profile were generated by GraphPad Prism software. Data analyzed by paired T-test n represents the number of subjects.

The human T cells lose an average of 50 base pairs of telomeric DNA per cell division. The activity of telomerase replenishes the telomeres. The human telomerase comprises a catalytic portion-human telomerase reverse transcriptase (hTERT) and the telomerase RNA (TR), which is the RNA component. Evaluation of the telomerase activity is a commonly used molecular tool in understanding the possible mechanisms of T cell senescence. To this end, we examined the gene expression levels of telomerase by RT-PCR and telomerase activity by the telomeric repeat amplification protocol (TRAP) assay in $CD4^+$ T cells exposed to ICRF-193 and compared it to DMSO control. As shown in fig. 15, while there was no significant difference in telomerase

expression levels in the Top2a-inhibited cells, there was a significant inhibition in telomerase activity, recapitulating what was observed in chronic HBV, HCV, and HIV infection.

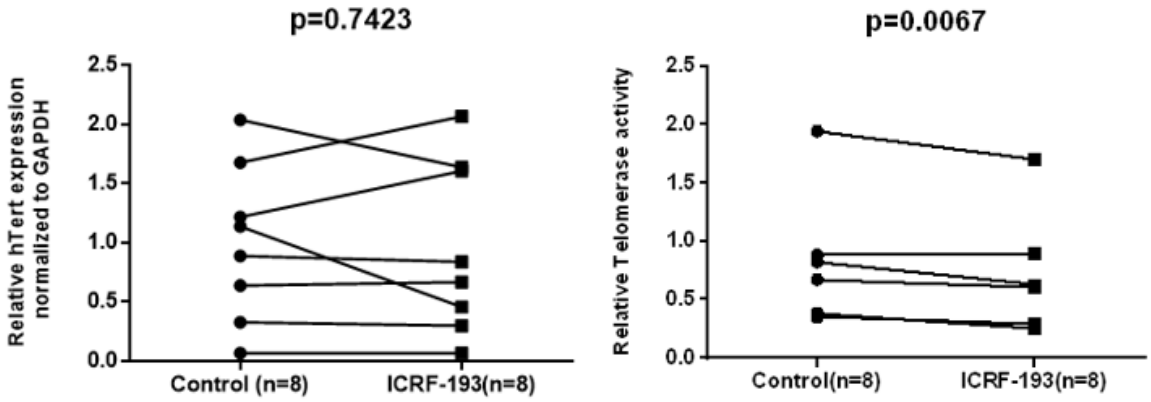

Figure 15. Effect of Top2α inhibition on telomerase activity. Relative hTERT expression measured by RT-qPCR and telomerase activity measured by TRAP assay in ICRF193 treated cells versus DMSO control. n represents the number of subjects.

Top2α-mediated DNA Damage Suppresses the DNA Damage repair kinase Ataxia Telangiectasia-Mutated (ATM)

In response to double-stranded DNA damage, well-coordinated signaling repair pathways are activated to repair the damage. The initial response includes the upregulation of the activity of the cell cycle checkpoint genes and the halting of the cell cycle advancement. This allows time for the repair of DNA in the damaged cell. Failure of the cells to repair their double-stranded breaks lead to the activation of the DDR pathways by the phosphatidylinositol -3 kinase-related kinases (PIKK). The major kinases in this group are the ataxia telangiectasia-Mutated (ATM), ataxia telangiectasia and Rad3 Related (ATR), and DNA-dependent protein kinase c (DNA-PKcs); and they are crucial in maintaining genomic stability. While unrepaired single-stranded breaks lead primarily to the activation of ATR, ATM and DNA-PKcs are predominantly

activated in response to double-stranded DNA breaks. To this end, we explored the involvement of ATM in Top2α-mediated DNA damage. The expression profile of ATM was examined in TCR-stimulated $CD4^+$ cells exposed to DMSO (control) and (ICRF193 treatment) at different time points (6h, 24h, 48h, and 72h) by western blotting. As shown in fig. 16, there was an increased expression of ATM in the early stage (6-24h) in response to DNA damage, followed by a gradual decline in the later phase (48h-72h) in ICRF-193-treated cells. This finding recapitulates what was observed in chronically HCV infected individuals.[33]

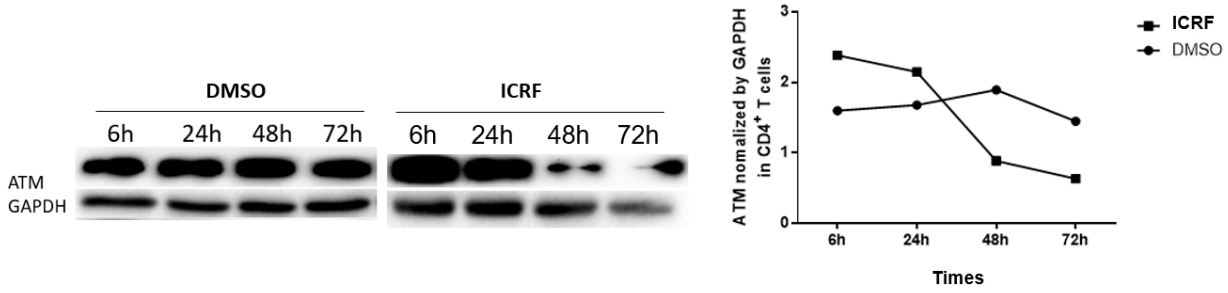

Figure 16. Expression kinetics of ATM in TCR-stimulated, Top2α-inhibited $CD4^+$ cells

Representative western blot image and summary data showing the time-point of ATM expression. $CD4^+$ T cells exposed to ICRF193 or DMSO control were cultured at different time points (6h, 24h, 48h, and 72h). GAPDH was used as the loading control. Protein band intensity was analyzed with ImageJ software. Summary data of ATM expression are generated by GraphPad Prism software.

CHAPTER 4

DISCUSSION

The goal of this study was to investigate the fundamental mechanism of telomeric DNA damage and immune evasion during chronic viral infections. Top2α removes supercoils and catenations during DNA related activities. Inhibition in the catalytic activity of Top2α leads to failure in the religation of the DNA backbone, and these transient breaks become converted to a permanent DNA break, which can be sensed as DNA damage and elicit the DNA damage response signals.

In this project, we hypothesized that viral infection might disrupt the topology of DNA as a means to evade the immune system and maintain persistence. We found that Top2α protein level was significantly suppressed in chronic HIV, HCV, and HBV subjects than healthy subjects. To determine the level at which this inhibition might have occurred, we examined the mRNA expression of Top 2α. We found that there was no change at the mRNA levels, suggesting that Top2α protein is inhibited primarily at the translation level. Also, the DNA damage induced by Top2α leads to apoptosis and T cell dysfunction, and mirrored what was observed in chronic HIV and HCV individuals. [32,33]

Top 2α expression level is notably upregulated in rapidly growing cells such as cancer cells, as these cells undergo fast gene replications, recombination, and thus tangling of the DNA backbone is prone to occur. Top 2α activity is essential to prevent mitotic failure and ensure adequate cell proliferation. In our study, we observed that chronic viral infection suppressed Top2α expression and activity, thereby making $CD4^+$ T cells dysfunctional and senescent. This indicates that adequate Top2α activity promotes T cell survival and function.

Another possible reason for the suppression of Top2α activity observed in this project could be that these viruses disrupt the mitochondrial function leading to an increase in the levels of reactive oxygen species (ROS). An increase in ROS generation may alter ATP levels, thereby making ATP unavailable for cellular processes. It is, therefore, pertinent to examine the mitochondrial kinetics in these cells.

Furthermore, we ascertained whether the DNA damage induced by Top2α inhibition was widespread within the DNA or it extended to the telomeres. Telomere shortening or dysfunction is a feature of premature T cell aging observed in chronic HIV or HCV infections. Our finding suggests that the DNA damage caused by Top2α inhibition indeed extends to the telomere as it disrupts the shelterin integrity, inhibits telomerase activity, and leads to an increase in the number of dysfunctional telomere induced foci (TIF), visualized by confocal microscopy.

Of the shelterin proteins, only TRF2 protein was significantly inhibited following Top2α inhibition. This suggests that TRF2 could be the significant shelterin protein affected by Top2a deficiency to cause telomeric DNA damage. This recapitulates the findings observed in individuals with chronic HCV infection. [33,35] While TRF2 degradation observed in chronic HCV individuals was noted to be due to a p53-dependent ubiquitin process; this pathway remained to be explored in the setting of Top2α inhibition. Also, the impact of TRF2 degradation on the mitochondrial function could be studied.

Surprisingly, while the level of the human telomerase reverse transcriptase (hTERT) remained unchanged, its activity was significantly suppressed following Top2α inhibition. Many reports have observed a significant correlation of hTERT expression with telomerase activity in some carcinomas; however, this was not in this case. Well, evidence accumulates on telomerase activity linked with only full-length mRNA transcripts, whereas other alternatively spliced

variants of hTERT mRNA could inhibit telomerase activity. Whether this is the case in our observation, remains to be explored.

In the event of DNA damage, the DNA repair kinases notably ATM are mobilized to the site of damage and phosphorylates downstream cell cycle checkpoint kinases CHK2 and CHK1. This halts the progression of the cell cycle and allows time for the damage to be repaired. In this study, we observed an initial induction of ATM expression in the early stages (6-24h) following ICRF-193 treatment and a gradual decline in expression in the later stages (48-72h). This finding is similar to what was observed in chronic HIV infected individuals. [55] Taken together, this could mean that ATM and TRF2 inhibition could be the key players involved in telomere dysfunction and cellular senescence during chronic viral infections.

The findings from this study provide evidence that HBV, HCV, and HIV viruses evade the immune response by disrupting the DNA topology of the T cell. Since we have proved that Top 2α expression and activity is suppressed, further studies aimed at exploring the possible pathways of Top2α degradation should be studied. Since the ubiquitin-proteasomal protein degradation pathway usually degrades most mutated or truncated proteins, it would not be out of place to confirm if a similar pathway mediates the degradation of Top2α. $CD4^+$ T cells from healthy subjects exposed to ICRF193 or etoposide could be treated with ubiquitin or proteasome inhibitor to see if Top 2α levels can be boosted. Similarly, Top2α overexpression experiments could be done in $CD4^+$ T cells from chronic HIV, HCV, and HBV subjects to establish if the DNA damage in these cells could be reversed.

REFERENCES

1. Burns GS, Thompson AJ. Viral Hepatitis B: Clinical and Epidemiological Characteristics. Cold Spring Harbor Perspectives in Medicine. 2014;4(12).

2. Bayer ME, Blumberg BS, Werner B. Particles associated with Australia antigen in the sera of patients with leukaemia, Down's Syndrome and hepatitis. Nature. 1968;218(5146):1057–1059.

3. Blumberg BS, Alter HJ. A New Antigen in Leukemia Sera. JAMA. 1965;191(7):541–546.

4. Blumberg BS, Sutnick AI, London WT. Hepatitis and leukemia: their relation to Australia antigen. Bulletin of the New York Academy of Medicine. 1968;44(12):1566–1586.

5. Hepatitis B. https://www.who.int/news-room/fact-sheets/detail/hepatitis-b

6. Harris AM. Increases in Acute Hepatitis B Virus Infections — Kentucky, Tennessee, and West Virginia, 2006–2013. MMWR. Morbidity and Mortality Weekly Report. 2016;65.

7. Gish RG, Given BD, Lai C-L, Locarnini SA, Lau JYN, Lewis DL, Schluep T. Chronic hepatitis B: Virology, natural history, current management and a glimpse at future opportunities. Antiviral Research. 2015; 121:47–58.

8. Gómez-Moreno A, Garaigorta U. Hepatitis B Virus and DNA Damage Response: Interactions and Consequences for the Infection. Viruses. 2017;9(10):304.

9. Tu T, Budzinska MA, Vondran FWR, Shackel NA, Urban S. Hepatitis B Virus DNA Integration Occurs Early in the Viral Life Cycle in an In Vitro Infection Model via Sodium Taurocholate Cotransporting Polypeptide-Dependent Uptake of Enveloped Virus Particles. Journal of Virology. 2018;92(11): e02007-17.

10. Lamontagne RJ, Bagga S, Bouchard MJ. Hepatitis B virus molecular biology and pathogenesis. Hepatoma Research. 2016; 2:163–186.

11. Lamontagne RJ, Bagga S, Bouchard MJ. Hepatitis B virus molecular biology and pathogenesis. Hepatoma Research. 2016;2(7):163.

12. Feinstone SM, Kapikian AZ, Purcell RH, Alter HJ, Holland PV, Zuckerman R by AJ. Transfusion-associated hepatitis not due to viral hepatitis type A or B. Reviews in Medical Virology; Chichester. 2001;11(1):3.

13. Dewar TN. Non-A, Non-B Hepatitis. Western Journal of Medicine. 1990;153(2):173–179.

14. Seeff LB. The history of the "natural history" of hepatitis C (1968-2009). Liver International: Official Journal of the International Association for the Study of the Liver. 2009;29 Suppl 1:89–99.

15. Jafri S-M, Gordon SC. Epidemiology of Hepatitis C. Clinical Liver Disease. 2018;12(5):140–142.

16. Commentary | U.S. 2016 Surveillance Data for Viral Hepatitis | Statistics & Surveillance | Division of Viral Hepatitis | CDC. 2019 Feb 13. https://www.cdc.gov/hepatitis/statistics/2016surveillance/commentary.htm

17. Morozov VA, Lagaye S. Hepatitis C virus: Morphogenesis, infection and therapy. World Journal of Hepatology. 2018;10(2):186–212.

18. Li H-C, Lo S-Y. Hepatitis C virus: Virology, diagnosis and treatment. World Journal of Hepatology. 2015;7(10):1377–1389.

19. Sharp PM, Hahn BH. Origins of HIV and the AIDS Pandemic. Cold Spring Harbor Perspectives in Medicine: 2011;1(1).

20. Maartens G, Celum C, Lewin SR. HIV infection: epidemiology, pathogenesis, treatment, and prevention. The Lancet. 2014;384(9939):258–271.

21. HIV/AIDS. https://www.who.int/news-room/fact-sheets/detail/hiv-aids

22. WHO | Data and statistics. WHO. http://www.who.int/hiv/data/en/

23. Naif HM. Pathogenesis of HIV infection. Infectious Disease Reports. 2013;5(1S):6.

24. Chinen J, Shearer WT. Molecular virology and immunology of HIV infection. Journal of Allergy and Clinical Immunology. 2002;110(2):189–198.

25. Reese TA, Bi K, Kambal A, Filali-Mouhim A, Beura LK, Bürger MC, Pulendran B, Sekaly R, Jameson SC, Masopust D, et al. Sequential infection with common pathogens promotes human-like immune gene expression and altered vaccine response. Cell host & microbe. 2016;19(5):713–719.

26. Beura LK, Hamilton SE, Bi K, Schenkel JM, Odumade OA, Casey KA, Thompson EA, Fraser KA, Rosato PC, Filali-Mouhim A, et al. Recapitulating adult human immune traits in laboratory mice by normalizing environment. Nature. 2016;532(7600):512–516.

27. Balasubramaniam M, Pandhare J, Dash C. Immune Control of HIV. Journal of Life Sciences (Westlake Village, Calif.). 2019;1(1):4–37.

28. Tan A, Koh S, Bertoletti A. Immune Response in Hepatitis B Virus Infection. Cold Spring Harbor Perspectives in Medicine. 2015;5(8).

29. Shin H, Wherry EJ. CD8 T cell dysfunction during chronic viral infection. Current Opinion in Immunology. 2007;19(4):408–415.

30. Oldstone MBA. Anatomy of Viral Persistence Madhani HD, editor. PLoS Pathogens. 2009;5(7): e1000523.

31. Thimme R, Binder M, Bartenschlager R. Failure of innate and adaptive immune responses in controlling hepatitis C virus infection. FEMS Microbiology Reviews. 2012;36(3):663–683.

32. Yao ZQ, Moorman JP. Immune Exhaustion and Immune Senescence: Two Distinct Pathways for HBV Vaccine Failure During HCV and/or HIV Infection. Archivum Immunologiae et Therapiae Experimentalis. 2013;61(3):193–201.

33. Zhao J, Dang X, Zhang P, Nguyen LN, Cao D, Wang L, Wu X, Morrison ZD, Zhang Y, Jia Z, et al. Insufficiency of DNA repair enzyme ATM promotes naive CD4 T-cell loss in chronic hepatitis C virus infection. Cell Discovery. 2018;4(1):16.

34. Kim H, Li F, He Q, Deng T, Xu J, Jin F, Coarfa C, Putluri N, Liu D, Songyang Z. Systematic analysis of human telomeric dysfunction using inducible telosome/shelterin CRISPR/Cas9 knockout cells. Cell Discovery. 2017;3:17034.

35. Nguyen LN, Zhao J, Cao D, Dang X, Wang L, Lian J, Zhang Y, Jia Z, Wu XY, Morrison Z, et al. Inhibition of TRF2 accelerates telomere attrition and DNA damage in naïve CD4 T cells during HCV infection. Cell Death & Disease. 2018;9(9):900.

36. Liu L, Trimarchi JR, Navarro P, Blasco MA, Keefe DL. Oxidative stress contributes to arsenic-induced telomere attrition, chromosome instability, and apoptosis. The Journal of Biological Chemistry. 2003;278(34):31998–32004.

37. Lange T de. Shelterin: the protein complex that shapes and safeguards human telomeres. Genes & Development. 2005;19(18):2100–2110.

38. Newman JPA, Banerjee B, Fang W, Poonepalli A, Balakrishnan L, Low GKM, Bhattacharjee RN, Akira S, Jayapal M, Melendez AJ, et al. Short dysfunctional telomeres impair the repair of arsenite-induced oxidative damage in mouse cells. Journal of Cellular Physiology. 2008;214(3):796–809.

39. Fumagalli M, Rossiello F, Clerici M, Barozzi S, Cittaro D, Kaplunov JM, Bucci G, Dobreva M, Matti V, Beausejour CM, et al. Telomeric DNA damage is irreparable and causes persistent DNA damage response activation. Nature cell biology. 2012;14(4):355–365.

40. Nitiss JL. DNA topoisomerase II and its growing repertoire of biological functions. Nature Reviews Cancer. 2009;9(5):327–337.

41. Champoux JJ. DNA Topoisomerases: Structure, Function, and Mechanism. Annual Review of Biochemistry. 2001;70(1):369–413.

42. Deweese JE, Osheroff N. The DNA cleavage reaction of topoisomerase II: wolf in sheep's clothing. Nucleic Acids Research. 2009;37(3):738–748.

43. Wang Y-R, Chen S-F, Wu C-C, Liao Y-W, Lin T-S, Liu K-T, Chen Y-S, Li T-K, Chien T-C, Chan N-L. Producing irreversible topoisomerase II-mediated DNA breaks by site-specific Pt(II)-methionine coordination chemistry. Nucleic Acids Research. 2017;45(18):10861–10871.

44. Nikitina T, Norouzi D, Grigoryev SA, Zhurkin VB. DNA topology in chromatin is defined by nucleosome spacing. Science Advances. 2017;3(10):e1700957.

45. Pommier Y, Sun Y, Huang S-YN, Nitiss JL. Roles of eukaryotic topoisomerases in transcription, replication and genomic stability. Nature Reviews. Molecular Cell Biology. 2016;17(11):703–721.

46. Infante Lara L, Fenner S, Ratcliffe S, Isidro-Llobet A, Hann M, Bax B, Osheroff N. Coupling the core of the anticancer drug etoposide to an oligonucleotide induces topoisomerase II-mediated cleavage at specific DNA sequences. Nucleic Acids Research. 2018;46(5):2218–2233.

47. Ali Y, Abd Hamid S. Human topoisomerase II alpha as a prognostic biomarker in cancer chemotherapy. Tumour Biology: The Journal of the International Society for Oncodevelopmental Biology and Medicine. 2016;37(1):47–55.

48. Abu Saleh M, Solayman M, Hoque MM, Khan MAK, Sarwar MG, Halim MA. Inhibition of DNA Topoisomerase Type IIα (TOP2A) by Mitoxantrone and Its Halogenated Derivatives: A Combined Density Functional and Molecular Docking Study. BioMed Research International. 2016

49. Jadhav AK, Karuppayil SM. Molecular docking studies on thirteen fluoroquinolines with human topoisomerase II a and b. In Silico Pharmacology. 2017;5(1):4.

50. Jain CK, Majumder HK, Roychoudhury S. Natural Compounds as Anticancer Agents Targeting DNA Topoisomerases. Current Genomics. 2017;18(1):75–92.

51. Ahmed SM, Dröge P. Oncofetal HMGA2 attenuates genotoxic damage induced by topoisomerase II target compounds through the regulation of local DNA topology. Molecular Oncology. 2019;13(10):2062–2078.

52. Hevener KirkE, Verstak TA, Lutat KE, Riggsbee DL, Mooney JW. Recent developments in topoisomerase-targeted cancer chemotherapy. Acta Pharmaceutica Sinica. B. 2018;8(6):844–861.

53. Nitiss JL. Targeting DNA topoisomerase II in cancer chemotherapy. Nature reviews. Cancer. 2009;9(5):338–350.

54. An X, Xu F, Luo R, Zheng Q, Lu J, Yang Y, Qin T, Yuan Z, Shi Y, Jiang W, et al. The prognostic significance of topoisomerase II alpha protein in early stage luminal breast cancer. BMC Cancer. 2018;18.

55. Yao ZQ, Zhao J, Nguyen LNT, Nguyen LN, Dang X, Cao D, Khanal S, Schank M, Chand Thakuri BK, Morrison ZD, et al. ATM deficiency accelerates DNA damage, telomere erosion, and premature T cell aging in HIV-infected individuals on antiretroviral therapy. Frontiers in Immunology. 2019;10.

VITA

STELLA CHINYERE OGBU

Education:	Master of Science in Biology, East Tennessee State University, Biological Sciences Department, 2019
	Bachelor of Medicine, Bachelor of Surgery, Abia State University Uturu, Nigeria, 2013
Professional Experience:	Graduate Assistant, East Tennessee State University, Biological Science Department, 2019